
DATA-EFFICIENT VISUOMOTOR POLICY TRAINING USING REINFORCEMENT LEARNING AND GENERATIVE MODELS

***Ali Ghadirzadeh**^{1,2}

algh@kth.se

***Petra Poklukar**,¹

poklukar@kth.se

Ville Kyrki²

ville.kyrki@aalto.fi

Danica Kragic¹

dani@kth.se

Mårten Björkman¹

celle@kth.se

¹ Division of Robotics, Perception and Learning

KTH Royal Institute of Technology, Stockholm, Sweden

² Intelligent Robotics Research Group

Aalto University, Espoo, Finland

* These authors contributed equally

The work is in progress

ABSTRACT

We present a data-efficient framework for solving deep visuomotor sequential decision-making problems which exploits the combination of reinforcement learning (RL) with the latent variable generative models. Our framework trains deep visuomotor policies by introducing an action latent variable such that the feed-forward policy search can be divided into two parts: (1) training a sub-policy that outputs a distribution over the action latent variable given a state of the system, and (2) training a generative model that outputs a sequence of motor actions given a latent action representation. Our approach enables safe exploration and alleviates the data-inefficiency problem as it exploits prior knowledge about valid sequences of motor actions. Moreover, by evaluating the quality of the generative models we are able to predict the performance of the RL policy training prior to the actual training on the physical robot. We achieve this by defining two novel measures, disentanglement and local linearity, for assessing the quality of generative models' latent spaces, and complementing them with the existing measures for evaluation of generative models. We demonstrate the efficiency of our approach on a picking task using several different generative models and determine which of their properties have the most influence on the final policy training.

1 Introduction

Reinforcement learning (RL) can leverage the modeling capability of generative models to solve complex sequential decision making problems more efficiently. RL has been applied to end-to-end training of deep visuomotor robotic policies [1, 2] but it is typically too data-inefficient especially when applied to the tasks that provide only a terminal

reward at the end of an episode. One way to alleviate the data-inefficiency problem in RL is by leveraging prior knowledge to reduce the complexity of the optimization problem. One prior that significantly reduces the temporal complexity is an approximation of the distribution from which valid action sequences can be sampled. Such distributions can be efficiently approximated by training generative models given a sufficient amount of valid action sequences.

The question is then how to combine the powerful RL optimization algorithms with the great modeling capability of the generative models to improve the efficiency of the policy training? Moreover, which characteristics of the generative models are important for the efficient policy training? A suitable generative model must capture the widest distribution of the training data to generate as many distinct motion trajectories as possible while avoiding the generation of invalid trajectories outside the training dataset. The diversity of the generated data enables the policy to complete a given task for a wider set of target states. On the other hand, adhering to the distribution of the training data ensures safety in generating trajectories which are running on a real-robotic platform.

In this paper, we (1) exploit RL to train a deep visuomotor policy that combined with a generative model generates feed-forward sequences of motor commands to control a robotic arm given image pixels as the input, and (2) provide a set of measures, two of which introduced by us, to evaluate the quality of the latent space of different generative models when regulated by the RL policy search algorithms.

Regarding (1), we propose a learning framework that divides the deep visuomotor sequential decision-making problem into the following sub-problems that can be solved more efficiently: (a) an unsupervised generative model training problem that approximates the distribution of motor actions, (b) a trust-region policy optimization problem that solves a contextual multi-armed bandit without temporal complexities, and (c) a supervised learning problem that trains the deep visuomotor policy in an end-to-end fashion.

Regarding (2), we evaluate generative models based on (a) the quality and coverage of the samples they generate using the precision and recall metric [3, 4], and (b) the quality of their latent representations using our novel measures of *disentanglement* and *local linearity*. Both of our metrics leverage the end states obtained after execution of the generated trajectories on a robotic platform. Disentanglement measures to which extend separate sets of dimensions in the latent space control different aspects of the task, while local linearity measures the complexity of the generative process and system dynamics in the neighbourhood of each latent representation. Our hypothesis is that a generative model that is well disentangled, locally linear and able to generate realistic samples that closely follow the training data (i.e. has high precision and high recall) leads to a more efficient neural network policy training. We experimentally investigate this hypothesis on several generative models, namely β -VAEs [5] and InfoGANs [6], and use automatic relevance determination regression (ARD) to quantify the effect of each characteristic on the RL policy training performance.

In summary, the advantages of our framework are:

- It improves data-efficiency of the policy training algorithm by incorporating the prior knowledge in terms of a distribution over valid sequences of actions, therefore, reducing the search space.
- It helps to acquire complex visuomotor policies given sparse terminal rewards provided at the end of a successful episode. The proposed formulation converts the sequential decision-making problem into a contextual multi-armed bandit without time complexities. Therefore, it alleviates the temporal credit assignment problem that is inherent in the sequential decision-making tasks which enables efficient policy training with only terminal rewards.
- It enables safe RL exploration by sampling actions only from the approximated distribution. This is in stark contrast to the typical RL algorithms in which random actions are taken during the exploration phase.
- It provides a set of measures for evaluation of the generative model based on which it is possible to predict the performance of the RL policy training task prior to the actual training.

This paper provides a comprehensive overview of our earlier work for RL policy training based on generative models [7–11] and is organized as follows: in Section 2, we provide an overview of the related work. We formally introduce the

problem of policy training with generative models in Section 3, and describe how the framework is trained in Section 4. In Section 5 we first briefly overview VAEs and GANs, and then define all of the evaluation measures used to predict the final policy training performance. Section 6 describes the end-to-end training of the perception and control modules. We present the experimental results in Section 7. Finally, the conclusions and future work are provided in Section 8.

2 Related work

Our work addresses two types of problems: (1) visuomotor policy training based on unsupervised generative model training and trust-region policy optimization, and (2) evaluation of generative models to forecast the efficiency of the final policy training task. We introduce the related work for each of the problems in the following sections.

2.1 Data-efficient End-to-end Policy Training

In recent years, end-to-end training of visuomotor policies using deep reinforcement learning has gained in popularity in robotics research [1, 7, 12–17]. However, deep RL algorithms are typically very data-hungry and learning a general policy, i.e., a policy that performs well also for previously unseen inputs, requires a farm of robots continuously collecting data for several days [2, 18–20]. The limitation of large-scale data collection has hindered the applicability of RL solutions to many practical robotics tasks. Recent studies tried to improve the data-efficiency by training the policy in simulation and transferring the acquired visuomotor skills to the real setup [14, 17, 21, 22], a paradigm known as sim-to-real transfer learning. Sim-to-real approaches are utilized for two tasks in deep policy training, (1) training the perception model via randomization of the texture and shape of visual objects in simulation and using the trained model directly in the real world setup (zero-shot transfer) [10, 23], and (2) training the policy in simulation by randomizing the dynamics of the task and transferring the policy to the real setup by fine-tuning it with the real data (few-shot transfer learning) [8, 22]. However, challenges in the design of the simulation environment can cause large differences between the real and the simulated environments which hinder an efficient transfer knowledge between these two domains. In such cases, transfer learning from other domains, e.g., human demonstrations [11, 24] and simpler task setups [9, 25] can help the agent to learn a policy more efficiently. In this work, we exploit human demonstration to shape the robot motion trajectories by training generative models that reproduce the demonstrated trajectories. Following our earlier work [9], we exploit adversarial domain adaptation techniques [26, 27] to improve the generality of the acquired policy when the policy is trained in a simple task environment with a small amount of training data. In the rest of this section, we review related studies that improve the data-efficiency and generality of RL algorithms by utilizing trust-region terms, converting the RL problem into a supervised learning problem, and trajectory-centered approaches that shape motion trajectories prior to the policy training.

Schulman et al. introduced two policy gradient methods, trust-region policy optimization (TRPO) [28] and proximal policy optimization (PPO) [29], that scale well to non-linear policies, such as neural networks. The key component of TRPO and PPO is a surrogate objective function with a trust-region term based on which the policy can be updated and monotonically improved while the policy distribution is not abruptly changed after each iteration. In TRPO, the changes in the distributions of the policies before and after each update are penalized by a KL divergence term. Therefore, the policy is forced to stay in a trust-region given by the action distribution of the current policy. Our EM formulation yields a similar trust-region term with the difference being that it penalizes the changes in the distribution of the deep policy and a so-called variational policy that will be introduced as a part of our proposed optimization algorithm. Since our formulation allows the use of any policy gradient solution, we use the same RL objective function.

EM algorithm has been used for policy training in a number of prior work, e.g., by Neumann [30], Deisenroth et al., [31], and Levine and Koltun [32]. The key idea is to introduce variational policies to decompose the policy training into two downstream tasks that are trained iteratively until no further policy improvement can be observed [33]. In a more recent work, Levine et al. [1] introduced guided policy search (GPS) algorithm which divides the visuomotor policy training task into a trajectory optimization and a supervised learning problem. GPS alternates between two steps:

(1) optimizing a set of trajectories by exploiting a trust-region term to stay close to the action distribution given by the deep policy, and (2) updating the deep policy to reproduce the motion trajectories. Our EM solution differs from the GPS framework and earlier approaches in that we optimize the trajectories by regulating a generative model that is trained prior to the policy training. Training generative models enables the learning framework to exploit human expert knowledge as well as to optimize the policy given only terminal rewards as explained earlier.

Trajectory-centric approaches, such as dynamic movement primitives (DMPs), have been popular because of the ease of integrating expert knowledge in the policy training process via physical demonstration [34–38]. However, such models are less expressive compared to deep neural networks and are particularly limited when it comes to the end-to-end training of the perception and the control elements of the model. Moreover, these approaches cannot be used to train reactive policies where the action is adjusted in every time-step based on the observed sensory input [39]. On the other hand, deep generative models can model complex dependencies within the data by learning the underlying data distribution from which realistic samples can be obtained. Furthermore, generative models can be easily accommodated in larger neural networks without affecting the data integrity. Our framework based on generative models enables training both feedback (reactive) and feedforward policies by adjusting the policy network architecture.

The use of generative models in policy training has become popular in recent years [7–11, 40–48] because of their low-dimensional and regularized latent spaces. However, latent variable generative models are mainly studied to train a long-term state prediction model that is used in the context of trajectory optimization and model-based reinforcement learning [43–48]. Regulating generative models based on reinforcement learning to produce sequences of actions according to the visual state has first appeared in our prior work [7]. Since then we applied the framework in different robotic tasks, e.g., throwing balls [7], shooting hockey-pucks [8], pouring into mugs [9, 10], and in a variety of problem domains, e.g., sim-to-real transfer learning [8, 10] and domain adaptation to acquire general policies [9]. This work is a comprehensive study that builds the theoretical foundation of our earlier work and in addition studies the characteristics of the generative models that can affect the efficiency of the policy training task.

2.2 Evaluation of Generative Models

Although generative models have proved successful in many domains [40, 49–52] assessing their quality remains a challenging problem [53]. It involves analysing the quality of both latent representations and generated samples. A general belief is that a superior model possesses well structured latent space and tightly matches the distribution of the training data.

A widely adopted approach for assessing the quality of the latent representations is the measure of disentanglement [54, 55]. A representation is said to be disentangled if each latent component encodes exactly one ground truth generative factor present in the data [56]. Existing frameworks for both learning and evaluating disentangled representations [5, 56–58] rely on the assumption that the ground truth factors of variation are known a priori and are independent. Their core idea is to measure how changes in the generative factors affect the latent representations and vice versa. In cases when an encoder network is available, this is typically achieved with a classifier that was trained to predict which generative factor was held constant given a latent representation. In generative models without an encoder network, such as GANs, disentanglement is measured by visually inspecting the latent traversals provided that the input data are images [6, 59–61]. However, these measures are difficult to apply when generative factors of variation are unknown or when manual visual inspection is not possible, both of which is the case with sequences of motor commands for controlling a robotic arm. We therefore define a measure of disentanglement that does not rely on any of these requirements and instead leverages the end states of the downstream robotics task corresponding to a given set of latent action representation. In contrast to the existing measures it measures how changes in the latent space affect the obtained end states in a fully unsupervised way.

Assessing the quality of the learned distribution and samples from it presents a separate challenge. Generated samples and their variation should resemble those obtained from the training data distribution. Early developed metrics such as

IS [62], FID [63] and KID [64] provided a promising start but were shown to be unable to separate between failure cases, such as mode collapse or unrealistic generated samples. Instead of using one-dimensional score, [4] propose to evaluate the learned distribution by comparing the samples from it with the ground truth training samples using the notion of precision and recall. Intuitively, precision measures the similarity between the generated and real samples, while recall determines the fraction of the true distribution that is covered by the distribution learned by the model. The measure was further improved both theoretically and practically by [65], while [3] provides an explicit non-parametric variant of the original probabilistic approach.

3 Preliminaries

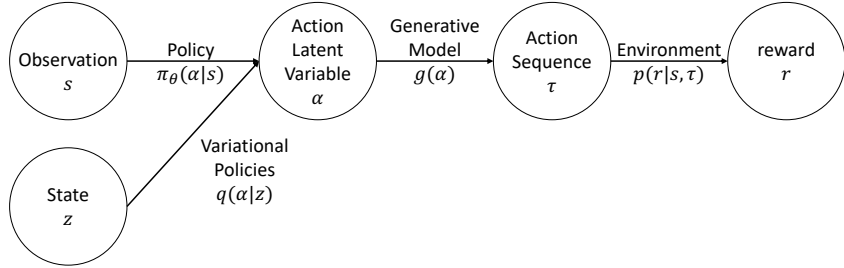


Figure 1: The architecture of the action-selection policy based on latent variable generative models.

Our framework consists of three parts: (1) policy training using EM algorithm combined with generative models, (2) training and evaluation of the generative models, and (3) training of the perception module. In this section, we introduce the problem of training a feed-forward deep policy network and describe our approach to solving it by leveraging generative models. We then present each of the three parts of the framework in the following section.

We deal with episodic tasks where the goal is to find a sequence of actions $\tau = \{a_{t,m}\} \in \mathbb{R}^{T \times M}$ consisting of T time-steps and M motor actions for a given state $s \in \mathbb{R}^{N_s}$. More specifically, we wish to find a policy $\pi_\Theta(\tau|s)$, represented by a deep neural network Θ , based on which a sequence of motor actions τ can be sampled given a state of the environment s . A state contains information about the current configuration of the environment as well as the goal to reach in case a goal-conditioned policy has to be obtained. For a given state s and a sequence of actions τ a reward r is given at the end of each trial according to the reward probability distribution $p(r|s, \tau)$ which is unknown to the learning agent. The policy π_Θ is represented by a neural network with parameters Θ that are trained to maximize the log-likelihood of receiving high rewards

$$\begin{aligned} \Theta^* &= \operatorname{argmax}_{\Theta} \iint p(s) \pi_\Theta(\tau|s) p(r|s, \tau) ds d\tau \\ &= \operatorname{argmax}_{\Theta} \mathbb{E}_{s \sim p(s), \tau \sim \pi_\Theta(\cdot|s)} [p(r|s, \tau)], \end{aligned} \tag{1}$$

where $p(s)$ denotes the distribution over states.

Our approach is based on training a generative model g_ϑ , parametrized by ϑ , that maps a low-dimensional latent action variable $\alpha \in \mathbb{R}^{N_\alpha}$ into a motion trajectory $\tau \in \mathbb{R}^{T \times M}$ where $N_\alpha \ll T \times M$. In other words, we assume that the search space is limited to the trajectories spanned by the generative model. In this case, the feed-forward policy search problem splits into two sub-problems: (1) finding the mapping $g_\vartheta(\alpha)$ and (2) finding the sub-policy $\pi_\vartheta(\alpha|s)$, where $\Theta = [\theta, \vartheta]$. In the rest of the text we refer to the sub-policy as the *policy* and omit the parameters ϑ from the notation g_ϑ when they are not relevant. Instead of marginalizing over trajectories as in Eq. (1) we marginalize over the latent

variable by exploiting the generative model

$$\theta^* = \operatorname{argmax}_{\theta} \mathbb{E}_{s \sim p(s), \alpha \sim \pi_{\theta}(\cdot|s)} [p(r|s, g(\alpha))]. \quad (2)$$

Once the models are trained the policy output is found by first sampling from the policy $\alpha \sim \pi_{\theta}(\cdot|s)$ and then using the mapping g to get the sequence of motor actions $\tau = g(\alpha)$. There are four advantages to perform the policy search in the low-dimensional latent space: (1) the search space is considerably smaller compared to the high-dimensional trajectory space, (2) the sequential decision making problem is reduced to a contextual multi-armed bandit without temporal complexities and credit assignment problem, (3) the exploration is done based on trajectories generated by the generative model which increases the safety of real robot explorations, (4) it provides a natural way to provide prior knowledge based on human demonstration or general trajectory planning algorithms.

In the following section, we introduce the expectation-maximization algorithm for training an action-selection policy using a generative model based on which different motor trajectories suitable for solving a given task can be generated.

4 Expectation-Maximization Policy Training

We use the EM algorithm to find an optimal policy $\pi_{\theta^*}(\alpha|s)$. We first introduce a variational policy $q(\alpha|s)$ which is a simpler auxiliary distribution used to improve the training of π_{θ} . As the goal is to maximize the reward probability $p(r|s)$ we start by expressing its logarithm as $\log p(r|s, \tau) = \int q(\alpha|s) \log p(r|\alpha) d\alpha$, where we used the identity $\int q(\alpha|s) d\alpha = 1$ and omitted the conditioning on τ in the reward probability $p(r|\alpha)$ for simplicity. Following the EM derivation introduced in [30] and using the identity $p(r|s) = p(r, \alpha|s)/p(\alpha|r, s)$, the expression can be further decomposed into

$$\log p(r|s) = \underbrace{\int q(\alpha|s) \log \frac{p(r, \alpha|s)}{q(\alpha|s)} d\alpha}_{\text{I}} + \underbrace{\int q(\alpha|s) \log \frac{q(\alpha|s)}{p(\alpha|r, s)} d\alpha}_{\text{II}} \quad (3)$$

The second term (II) is the Kullback-Leibler (KL) divergence $D_{KL}(q(\alpha|s) || p(\alpha|r, s))$ between distributions $q(\alpha|s)$ and $p(\alpha|r, s)$, which is a non-negative quantity. Therefore, the first term (I) provides a lower-bound for $\log p(r|s)$. To maximize the latter we use the EM algorithm which is an iterative procedure consisting of two steps known as the expectation (E-) and the maximization (M-) steps, introduced in the following sections.

4.1 Expectation step

The E-step maximizes $\log p(r|s)$ by minimizing the KL divergence term (II) in Eq. (3). Since $\log p(r|s)$ does not depend on $q(\alpha|s)$ the sum of the KL divergence term (II) and the lower bound term (I) is a constant value for different q . Therefore, reducing (II) by optimizing q increases the lower bound (I). Assuming that q is parametrized by ϕ the E-step objective function is given by

$$\begin{aligned} \phi^* &= \operatorname{argmin}_{\phi} D_{KL}(q_{\phi}(\alpha|s) || p(\alpha|r, s)) \\ &= \operatorname{argmax}_{\phi} \mathbb{E}_{\alpha \sim q_{\phi}(\alpha|s)} [\log p(r|\alpha, s)] - D_{KL}(q_{\phi}(\alpha|s) || \pi_{\theta}(\alpha|s)), \end{aligned} \quad (4)$$

where we used the Bayes rule $p(\alpha|r, s) = p(r|\alpha, s)p(\alpha|s)/p(r|s)$ and substituted $p(\alpha|s)$ by $\pi_{\theta}(\alpha|s)$. In typical RL applications we assume that the reward is given by a deterministic reward function $r(s, \tau) = r(s, g(\alpha))$. In this case, $\mathbb{E}_{q_{\phi}(\alpha|s)} [\log p(r|\alpha, s)]$ can be maximized indirectly by maximizing the expected reward value $\mathbb{E}_{q_{\phi}(\alpha|s)} [r(s, \alpha)]$ on which we can apply the policy gradient theorem. Moreover, $D_{KL}(q_{\phi}(\alpha|s) || \pi_{\theta}(\alpha|s))$ acts as a trust region term forcing q_{ϕ} not to deviate too much from the policy distribution π_{θ} . Therefore, we can apply policy search algorithms

with trust region terms to optimize the objective given in Eq. (4). Following the derivations introduced in [28], we adopt TRPO objective for the E-step optimization

$$\phi^* = \operatorname{argmax}_{\phi} \mathbb{E}_{s \sim p(s), \alpha \sim \pi_{\theta}(\cdot|s)} \left[\frac{q_{\phi}(\alpha|s)}{\pi_{\theta}(\alpha|s)} A(s, \alpha) - D_{KL}(q_{\phi}(\alpha|s) \parallel \pi_{\theta}(\alpha|s)) \right], \quad (5)$$

where $A(s, \alpha) = r(s, \alpha) - V_{\pi}(s)$ is the advantage function, $V_{\pi}(s) = \mathbb{E}_{s \sim p(s), \alpha \sim \pi_{\theta}(\cdot|s)} [r(s, \alpha)]$ is the value function and ϕ^* denotes the optimal solution for the given iteration. Note that the action latent variable α is always sampled from the policy $\pi_{\theta}(\cdot|s)$ and not from the variational policy $q_{\phi}(\cdot|s)$.

4.2 Maximization step

The M-step directly maximizes the lower bound (I) in Eq. (3) by optimizing the policy parameters θ while holding the variational policy q_{ϕ} constant. Following [31] and noting that the dynamics of the system $p(r|\alpha, s)$ are not affected by the choice of the policy parameters θ , we maximize (I) by minimizing the following KL divergence

$$\theta^* = \operatorname{argmin}_{\theta} D_{KL}(q_{\phi}(\alpha|s) \parallel \pi_{\theta}(\alpha|s)). \quad (6)$$

In other words, the M-step updates the policy π_{θ} to match the distribution of the variational policy q_{ϕ} which was updated in the E-step. Similarly as in the E-step, θ^* denotes the optimal solution for the given iteration.

A summary of the EM policy training is given in Algorithm 1. In each iteration, a set of states is sampled from the state distribution $p(s)$. For each state s a latent action variable α is sampled from the distribution given by the policy $\pi_{\theta}(\cdot|s)$. A generative model g is then used to map every latent action variable α into a full motor trajectory τ which is then deployed on the robot to get the corresponding reward value. In the inner loop, the variational policy q_{ϕ} and the main policy π_{θ} are updated iteratively on batches of data using the objective function for the E- and M-steps of the policy optimization method.

Input : generative model g_{θ} , initial policy π_{θ} , initial value function V_{π} , batch size N

Output : trained π_{θ}

while training π_{θ} **do**

for $i = 1, \dots, N$ **do**

 sample states $s_i \sim p(s)$

 sample actions $\alpha_i \sim \pi_{\theta}(\cdot|s_i)$

 generate motor actions $\tau_i \leftarrow g_{\theta}(\alpha_i)$

 obtain the rewards $r_i \leftarrow r(s_i, \tau_i)$

repeat

E-step:

 update the variational policy q_{ϕ} according to Eq. (5) given $\{s_i, \alpha_i, r_i\}_{i=1}^N$

M-step:

 update the policy π_{θ} according to Eq. (6) given q_{ϕ} and $\{s_i, \alpha_i\}_{i=1}^N$

until training done;

 update the value function V_{π} given $\{s_i, r_i\}_{i=1}^N$

end

end

Algorithm 1: EM policy training based on generative models.

The number of variational policies can be chosen arbitrarily. We suggest to optimize several variational policies simultaneously in the E-step by splitting the state space into smaller sub spaces for each of which one variational policy is optimized. This can improve the efficiency of the policy training since variational policies with fewer parameters have to be optimized in a small region of the state space. The analysis of the effect of the number of the variational policies for the policy training is presented in Sec. 7.4.

5 Generative Model Training

So far we discussed how to train an action-selection policy based on the EM algorithm to regulate the action latent variable which is the input to a generative model. In this section we review two prominent approaches to train a generative model, VAE and GAN, which we use to generate sequences of actions required to solve the sequential decision-making problem. We then introduce a set of measures used to predict which properties of a generative model will influence the policy training.

5.1 Training generative models

We aim to model the true distribution $p(\tau)$ of the motor actions that are suitable to complete a given task. To this end, we introduce a low-dimensional random variable α with a probability density function $p(\alpha)$ representing the latent actions which are mapped into unique trajectories τ by a generative model g . The model g is trained to maximize the likelihood $\mathbb{E}_{\alpha \sim p(\alpha)}[p_\vartheta(\tau|\alpha)]$ of the training trajectories τ under the entire latent variable space.

5.1.1 Variational autoencoders

A VAE [66, 67] consists of an encoder and decoder neural networks representing the parameters of the approximate posterior distribution $q_\varphi(\alpha|\tau)$ and the likelihood function $p_\vartheta(\tau|\alpha)$, respectively. The encoder and decoder neural networks, parametrized by φ and ϑ , respectively, are jointly trained to optimize the variational lower bound

$$\max_{\varphi, \vartheta} \mathbb{E}_{\alpha \sim q_\varphi(\alpha|\tau)}[\log p_\vartheta(\tau|\alpha)] - \beta D_{KL}(q_\varphi(\alpha|\tau) || p(\alpha)), \quad (7)$$

where the parameter β [5] is a variable that controls the trade-off between the reconstruction fidelity and the structure of the latent space regulated by the KL divergence.

5.1.2 Generative adversarial networks

A GAN model [68] consists of a generator and discriminator neural networks that are trained by playing a minmax game. The generative model g_ϑ , parametrized by ϑ , transforms a latent variable α sampled from the prior noise distribution $p(\alpha)$ into a trajectory $\tau = g_\vartheta(\alpha)$. The model needs to produce realistic samples resembling those obtained from the training data distribution $p(\tau)$. It is trained by playing an adversarial game against the discriminator network D_φ , parametrized by φ , which needs to distinguish a generated sample from a real one. The competition between the two networks is expressed as the following minmax objective

$$\min_{\vartheta} \max_{\varphi} \mathbb{E}_{\tau \sim p(\tau)}[\log D_\varphi(\tau)] + \mathbb{E}_{\alpha \sim p(\alpha)}[\log(1 - D_\varphi(g_\vartheta(\alpha)))] \quad (8)$$

However, the original GAN formulation from Eq. (8) does not impose any restrictions on the latent variable α and therefore the generator g_ϑ can use α in an arbitrary way. To learn disentangled latent representations we instead use InfoGAN [6] which is a version of GAN with an information-theoretic regularization added to the original objective. The regularization is based on the idea to maximise the mutual information $I(\alpha, g_\vartheta(\alpha))$ between the latent code α and the corresponding generated sample $g_\vartheta(\alpha)$. An InfoGAN model is trained using the following information minmax objective [6]

$$\min_{\vartheta, \psi} \max_{\varphi} \mathbb{E}_{\tau \sim p(\tau)}[\log D_\varphi(\tau)] + \mathbb{E}_{\alpha \sim p(\alpha)}[\log(1 - D_\varphi(g_\vartheta(\alpha)))] - \lambda \mathbb{E}_{\alpha \sim p(\alpha), \tau \sim g_\vartheta(\alpha)}[\log Q_\psi(\alpha|\tau)], \quad (9)$$

where $Q_\psi(\alpha|\tau)$ is an approximation of the true unknown posterior distribution $p(\alpha|\tau)$ and λ a hyperparameter. In practice, Q_ψ is a neural network which shares all the convolutional layers with the discriminator network D_φ except for the last few output layers.

5.2 Evaluation of the generative models

We review the characteristics of generative models that can potentially improve the policy training by measuring precision and recall, disentanglement and local linearity. Our goal is to be able to judge the quality of the policy training by evaluating the generative models prior to the RL training. We relate the measures to the performance of the policy training in Section 7.2.

5.2.1 Precision and recall

Precision and recall for distributions is a measure, first introduced by [4] and further improved by [3], for evaluating the quality of a distribution learned by a generative model g . It is based on the comparison of samples obtained from g with the samples from the ground truth reference distribution. In our case, the reference distribution is the one of the training motor trajectories. Intuitively, *precision* measures the quality of the generated sequences of motor actions by quantifying how similar they are to the training trajectories. It determines the fraction of the generated samples that are realistic. On the other hand, *recall* evaluates how well the learned distribution covers the reference distribution and it determines the fraction of the training trajectories that can be generated by the generative model. In the context of the policy training, we would like the output of π_θ to be as similar as possible to the demonstrated motor trajectories. It is also important that π_θ covers the entire state space as it must be able to reach different goal states from different task configurations. Therefore, the generative model needs to have both high precision and high recall scores.

The improved measure introduced by [3] is based on an approximation of manifolds of both training and generated data. In particular, given a set $\mathbf{T} \in \{\mathbf{T}_r, \mathbf{T}_g\}$ of either real training trajectories \mathbf{T}_r or generated trajectories \mathbf{T}_g , the corresponding manifold is estimated by forming hyperspheres around each trajectory $\tau \in \mathbf{T}$ with radius equal to its k th nearest neighbour $\text{NN}_k(\tau, \mathbf{T})$. To determine whether or not a given novel trajectory τ' lies within the volume of the approximated manifold we define a binary function

$$f(\tau', \mathbf{T}) = \begin{cases} 1 & \text{if } \|\tau' - \tau\|_2 \leq \|\tau - \text{NN}_k(\tau, \mathbf{T})\|_2 \text{ for at least one } \tau \in \mathbf{T} \\ 0 & \text{otherwise.} \end{cases}$$

By counting the number of generated trajectories $\tau_g \in \mathbf{T}_g$ that lie on the manifold of the real data \mathbf{T}_r we obtain the *precision*, and similarly the *recall* by counting the number of real trajectories $\tau_r \in \mathbf{T}_r$ that lie on the manifold of the generated data \mathbf{T}_g

$$\text{precision}(\mathbf{T}_r, \mathbf{T}_g) = \frac{1}{|\mathbf{T}_g|} \sum_{\tau_g \in \mathbf{T}_g} f(\tau_g, \mathbf{T}_r) \quad \text{and} \quad \text{recall}(\mathbf{T}_r, \mathbf{T}_g) = \frac{1}{|\mathbf{T}_r|} \sum_{\tau_r \in \mathbf{T}_r} f(\tau_r, \mathbf{T}_g).$$

In our experiments, we use the original implementation provided by [3] directly on the trajectories as opposed to their representations as suggested in the paper.

5.2.2 Disentangled representation

In this section, we define our measure for evaluating the disentanglement of latent action representations. Disentangled representations obtained through unsupervised representation learning have shown to improve the learning efficiency of a large variety of downstream machine learning tasks [5, 6, 69]. We defined a representation of the motor data obtained from the latent space of a generative model as disentangled if every end state of the system is controllable by one latent dimension. For example, consider a reaching task where the goal is to reach different points in the Cartesian space. A well-disentangled representation given by a generative model forces each axis of the position of the end-effector to be controlled by one dimension of the latent variable. Our hypothesis is that the more disentangled the representation is, the more efficient is the policy training.

Our measure is based on statistical testing performed on the end state space of the system. Let \mathcal{S}_r the set of end states obtained by executing the training motor trajectories on a robotic platform. If representations given by g are well disentangled, then setting one latent dimension to a fixed value should result in limited variation in the corresponding generated end states \mathcal{S}_g . For example, if the 1st latent dimension controls the x -axis position of the end-effector in the reaching task then setting it to a fixed value should limit the set of possible x positions. In other words, we wish to quantify how dissimilar the set of end states \mathcal{S}_g , obtained by holding one latent dimension constant, is from the set \mathcal{S}_r . To compute such dissimilarity we use maximum mean discrepancy (MMD) [70] which is a statistical test for determining if two sets of samples were produced by the same distribution. Using kernels, MMD maps both sets into a feature space called reproducing kernel Hilbert space, and computes the distance between mean values of the samples in each group. In our implementations we compute the unbiased estimator of the squared MMD (Lemma 6 in [70]) given by

$$\text{MMD}^2(\mathcal{S}_r, \mathcal{S}_g) = \frac{1}{m(m-1)} \sum_{i \neq j}^m k(s_r^i, s_r^j) + \frac{1}{n(n-1)} \sum_{i \neq j}^n k(s_g^i, s_g^j) - \frac{2}{mn} \sum_{i=1}^m \sum_{j=1}^n k(s_r^i, s_g^j)$$

where $\mathcal{S}_r = \{s_r^1, \dots, s_r^m\}$, $\mathcal{S}_g = \{s_g^1, \dots, s_g^n\}$ are the two sets of samples and $k(x, y) = \exp(-\gamma \|x - y\|^2)$ is the exponential kernel with hyperparameter γ determining the smoothness. Due to the nature of the exponential kernel, the higher the MMD score, the lower the similarity between the two sets.

Our measure can be described in three phases. We provide an intuitive summary of each phase but refer the reader to Appendix A for a rigorous description of the algorithm. In phase 1 (Fig. 2 left) we generate the two sets of end states on which we run the statistical tests. For a fixed latent dimension $l \in \{1, \dots, N_\alpha\}$ we perform a series of $D \in \mathbb{N}$ *latent interventions* where we set the l th component of a latent code to a fixed value $\alpha_l = I_d$ for $d = 1, \dots, D$. Each intervention $\alpha_l = I_d$ is performed on a set of n samples sampled from the prior distribution $p(\alpha)$. We denote by $\mathcal{S}_g^{l-I_d}$ the set of n end states obtained by executing the trajectories generated from the intervened latent samples. For example, $D = 5$ latent interventions on the 1-st latent dimension yield the sets $\mathcal{S}_g^{1-I_1}, \dots, \mathcal{S}_g^{1-I_5}$. Moreover, we denote by \mathcal{S}_r the set of n randomly subsampled end states that correspond to the training motor data.

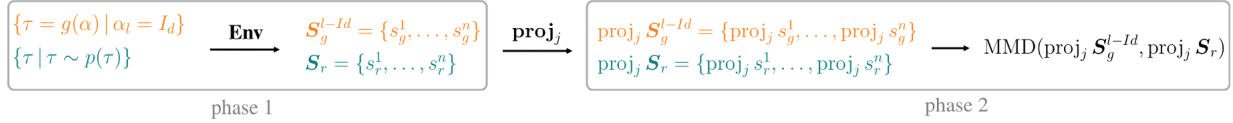


Figure 2: Visualisation of phase 1 and 2 of our disentanglement metric.

In phase 2 (Fig. 2 right), we perform the MMD tests on each pair of sets $\mathcal{S}_g^{l-I_d}$ and \mathcal{S}_r obtained in phase 1. In particular, we wish to determine if an intervention on a given dimension l induced a change in any of the components $j = 1, \dots, N_s$ of the end state space. If such a change exists, we consider the latent dimension l to be well disentangled. Moreover, if we can find a set of latent dimensions that induce changes on different components of the end states, we consider the generative model g to be well disentangled. Therefore, for a fixed latent dimension l and a fixed intervention $\alpha_l = I_d$, the objective is to find the component j of the end state space for which $\mathcal{S}_g^{l-I_d}$ and \mathcal{S}_r are most dissimilar. This translates to finding the component j yielding the largest value $\text{MMD}(\text{proj}_j \mathcal{S}_g^{l-I_d}, \text{proj}_j \mathcal{S}_r)$ where $\text{proj}_j \mathcal{S} = \{\text{proj}_j s \mid s \in \mathcal{S}\}$ denotes the set of the j th components of the states in \mathcal{S} . Note that if the dimension l is entangled such component j does not exist (see Appendix A for details).

In phase 3 we aggregate the values of the performed MMD tests and define the final disentanglement score for the generative model g . In phase 2 we linked each latent dimension l with zero or one end state component j and computed the corresponding value of the MMD test. Here, we first select $\min(N_s, N_\alpha)$ pairs with the largest MMD values. We define DiP(g) as the sum of the selected MMD values, and DiR(g) as the number of unique end state space components present in the selected pairs normalised by the total number of components N_s . Finally, we define the

Disentanglement Score DiS as a pair

$$\text{DiS}(g) = (\text{DiP}(g), \text{DiR}(g)).$$

Intuitively, $\text{DiP}(g)$ quantifies the effect of latent interventions on the end states and can therefore be thought of as *disentangling precision*. On the other hand, $\text{DiR}(g)$ measures how many different aspects of the end states are captured in the latent space and can be thus thought of as *disentangling recall*. The defined score is a novel fully unsupervised approximate measure of disentanglement for generative models combined with the RL policy training. Its absolute values can however vary depending on the kernel parameter γ determining its smoothness. Moreover, this measure is not to be confused with the precision and recall from Sec. 5.2.1 where the aim is to evaluate the quality of the generated samples as opposed to the quality of the latent representations.

5.2.3 Local linearity

The linearity of system dynamics plays a vital role in control theory but has not been studied in the context of generative model training. The system dynamics governs the evolution of the states as the result of applying a sequence of motor actions to the robot. Our hypothesis is that a generative model combined with the environment that satisfies the local linearity performs better in the policy training.

Let the mapping $\text{Env} : \mathbb{R}^{T \times M} \rightarrow \mathbb{R}^{N_s}$ represent the environment and let $s = \text{Env}(\tau) \in \mathbb{R}^{N_s}$ denote the state of the system after executing the actions τ . Let $N_\varepsilon(\alpha) = \{\alpha' : \|\alpha' - \alpha\|_2 < \varepsilon\}$ be the Euclidean ε -neighbourhood of a latent action α . Then the composition of the maps $\text{Env} \circ g : \mathbb{R}^{N_\alpha} \rightarrow \mathbb{R}^{N_s}$ mapping from the action latent space to the end state of the system is considered linear in the neighbourhood of α if there exists an affine transformation

$$\begin{aligned} f_\alpha : N_\varepsilon(\alpha) \subset \mathbb{R}^{N_\alpha} &\longrightarrow \mathbb{R}^D \\ \alpha' &\longmapsto A\alpha' + b \end{aligned} \tag{10}$$

such that $\text{Env}(g(\alpha')) = f_\alpha(\alpha')$ for every $\alpha' \in N_\varepsilon(\alpha)$. We measure the local linearity of a generative model g on a subset of latent actions $\{\alpha_i\}$ by calculating the mean square error (MSE) of f_{α_i} obtained on $N_\varepsilon(\alpha_i)$.

6 End-to-end Training of Perception and Control

The EM policy training algorithm presented in Sec. 4 updates the deep policy using the supervised learning objective function introduced in Eq. (6) (the M-step objective). Similar to guided policy search [1], the EM policy training formulation enables training of the perception and control parts of the deep policy together in an end-to-end fashion. In this section, we describe two techniques that can improve the efficiency of the end-to-end training.

6.1 Input remapping trick

The input remapping trick [1] can be applied to condition the variational policies q on a low-dimensional compact state representation, z , instead of the high-dimensional states s given by the sensory observations, e.g., camera images. The policy training phase can be done in a controlled environment such that extra measures other than the sensory observation of the system can be provided. These extra measures can be for example the position of a target object on a tabletop. Therefore, the image observations s can be paired with a compact task-specific state representation z such that z is used in the E-step for updating the variational policy $q(\alpha|z)$ and s in the M-step for updating the policy $\pi_\theta(\alpha|s)$.

6.2 Domain adaptation for perception training

The goal of this section is to exploit unlabeled images, captured without involving the robot, to improve the data-efficiency of the visuomotor policy training. Domain adaptation techniques, e.g., adversarial methods [9], can improve the end-to-end training of visuomotor policies with limited robot data samples. The unlabeled task-specific images are

exploited in the M-step to improve the generality of the visuomotor policy to manipulate novel task objects in cluttered backgrounds.

The M-step is updated to include an extra loss function to adapt data from the two different domains, (1) unlabeled images and (2) robot visuomotor data. The images must contain only one task object in a cluttered background, possibly different than the task object used by the robot during the policy training. Given images from the two domains, the basic idea is to extract visual features such that it is not possible to detect the source of the features. More details of the method can be found in our recent work in [9].

7 Experiments

In this section, we present our experimental results aimed at answering the following questions:

1. How does the proposed approach to divide the visuomotor policy training into several more manageable downstream tasks perform for end-to-end training of visuomotor policies?
2. Which of the characteristics precision and recall, disentanglement and local linearity of a generative model affect the policy training the most?
3. Does multi-agent training improve the efficiency of the policy training? What is the optimal number of the agents (i.e., variational policies) to speed up the training?

We answer (1) by training a deep visuomotor policy for a picking task on a real robotic platform. We demonstrate that a deep visuomotor policy can be trained after a few hundreds of trials that can be safely executed on a physical robot in less than 30 minutes. In this case, the visuomotor policy maps raw image pixel values to a complete sequence of motor actions to pick an object at different positions and orientations on a tabletop. By providing the results from our earlier study [9], we motivate the use of the introduced adversarial domain adaptation algorithm to improve the generality of the obtained deep visuomotor policy. The policy is general in the sense that it can manipulate novel task objects in a cluttered environment, a situation that has never been encountered during the policy training phase. We emphasize that our approach cannot be directly compared to neither PPO, since it requires vast amounts of data, nor GPS, since it requires a reward at every time step instead of the terminal reward as in our case.

We answer (2) by training several β -VAE and InfoGAN generative models with various hyperparameters and evaluate them using the measures introduced in Sec. 5.2. For each model, we train several RL policies based on the proposed EM algorithm and investigate how the performance is related to the discussed properties of the generative models.

Finally, we answer (3) by modifying the E-step of the EM algorithm to optimize for different number of variational policies. We choose a generative model that performed well in the single policy training task and evaluate the performance of the final policy training when deploying several variational policies. As the result, we can give the optimal number of variational policies that result in the best final policy training performance.

7.1 Experimental setup

We apply the framework to a picking task in which a 7 degree-of-freedom robotic arm (ABB YuMi) must move its end-effector to different positions and orientations on a tabletop to pick a randomly placed object on a table. This task is a suitable benchmark to answer our research questions. First of all, the task requires feed-forward controlling of the arm over 79 time-steps to precisely reach a target position without any position feedback during the execution. Therefore, precision is an important factor for this problem setup. Secondly, reaching a wide range of positions and orientations on the tabletop requires the generative model g to generate all possible combination of motor commands that bring the end-effector to every possible target position and orientation. This means that g needs to have a high recall. Thirdly, it is straightforward to evaluate the disentanglement of the latent representations as well as the local linearity of the dynamical system that is formed by g and the robot kinematic model. Finally, this is a suitable task for end-to-end

training, especially by exploiting the introduced adversarial domain adaptation technique to obtain generality for the policy training task.

Note that the applicability of our framework (up to minor differences) to a wide range of robotic problems has already been addressed by our prior work. In particular, we successfully evaluated it in several robotic task domains, e.g., ball throwing to visual targets [7], shooting hockey pucks using a hockey stick [8], pouring into different mugs [10], picking objects [9], and imitating human greeting gestures [11].

7.2 Generative model training

We construct a dataset containing sequences of motor actions using MoveIt default planner. We collected 15750 joint velocity trajectories to move the end-effector of the robot from a home position to different positions and orientations on a tabletop. The trajectories were sampled at 10Hz and trimmed to 79 time-steps (7.8 seconds duration) by adding zeros at the end of the joint velocities that are shorter than 79 time-steps. The target positions and orientations consisting of Euler angles form a $N_s = 6$ dimensional end state space, and were sampled uniformly to cover an area of $750 \text{ cm}^2 \times 3.1 \text{ rad}$.

The generative models are neural networks mapping a low-dimensional action latent variable into a 7×79 dimensional vector representing 7 motor actions and 79 time-steps. The input size of the networks is the same as the dimension of the latent space N_α . We refer the reader to the Appendix B for the exact architecture as well as all the training details. The prior distribution $p(\alpha)$ is assumed to be standard normal distribution $N(0, 1)$ in case of the VAEs, and uniform distribution $U(-1, 1)$ in case of the InfoGAN models.

In total, we trained 9 β -VAE models and 9 InfoGAN models. The VAEs were trained with different β parameters and latent sizes $N_\alpha \in \{2, 3, 6\}$. The parameters of each model together with the values of both the KL divergence term and the reconstruction term (right and left term in Eq. (7), respectively) are summarised in Table 1. At the beginning of the training we set $\beta = 0$ and gradually increase its value until the KL loss drops below a predetermined threshold set to 1.5, 2.5 and 3.5. The resulting β value is reported in Table 1 and kept fixed until the end of the training.

Table 2 summarizes the training parameters and loss function values of the InfoGAN models. We trained the models with latent sizes $N_\alpha \in \{2, 3, 6\}$ and $\lambda \in \{0.1, 1.5, 3.5\}$ (right term in Eq. (9)). We report the total model loss (Eq. (9)), the generator loss (middle term in Eq. (9)) and the mutual information loss (right term in Eq. (9)) obtained on the last epoch.

Table 1: VAE training and evaluation

index	latent size	β	KL loss	reconst. loss
VAE1	2	$1.6e - 2$	1.5	$2.1e - 2$
VAE2	2	$6.4e - 3$	2.5	$1.1e - 2$
VAE3	2	$3.2e - 3$	3.4	$6.7e - 3$
VAE4	3	$1.6e - 2$	1.5	$2.1e - 2$
VAE5	3	$7.2e - 3$	2.4	$1.1e - 2$
VAE6	3	$3.2e - 3$	3.5	$5.5e - 3$
VAE7	6	$1.6e - 2$	1.5	$2.1e - 2$
VAE8	6	$7.2e - 3$	2.4	$1.1e - 2$
VAE9	6	$3.6e - 3$	3.3	$6.0e - 3$

Table 2: InfoGAN training and evaluation

Model	latent size	λ	G-loss	I-loss	total loss
GAN1	2	0.1	2.81	0.10	0.54
GAN2	2	1.5	2.28	0.59	0.78
GAN3	2	3.5	2.43	1.07	0.63
GAN4	3	0.1	2.52	0.16	0.61
GAN5	3	1.5	2.27	1.45	0.75
GAN6	3	3.5	2.23	3.16	0.68
GAN7	6	0.1	2.50	0.44	0.63
GAN8	6	1.5	2.23	4.78	0.73
GAN9	6	3.5	2.27	10.32	0.67

7.3 Evaluating the generative models

We evaluated all the generative models based on precision and recall, disentanglement and local linearity measures described in Section 5.2.

Precision and recall For each generative model g we randomly sampled 15000 samples from the latent prior distribution $p(\alpha)$. The corresponding generated trajectories were compared with 15000 randomly chosen training trajectories which were sampled only once and fixed for all the models. The neighbourhood size k was set to 3 as suggested in [3]. The resulting precision and recall scores are shown in Figure 3.

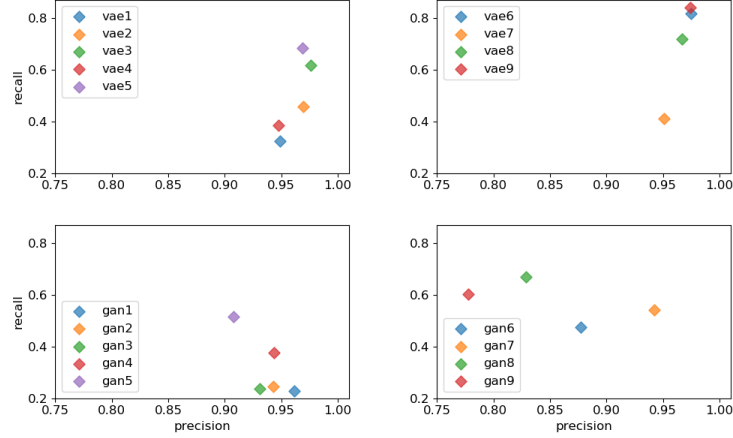


Figure 3: Precision and recall scores.

Disentanglement We measured the disentanglement using MMD with the kernel parameter $\gamma = 15$. For a given model g we performed $D = 5$ interventions on every latent dimension $l \in \{1, \dots, N_\alpha\}$. The size of the sets S_g^{l-Id} and S_r containing the end states was set to $n = 200$. For complete details we refer the reader to Appendix A. The obtained disentanglement scores are visualised in Figure 4.

Local linearity Given a generative model g we randomly sampled 50 latent actions from the prior $p(\alpha)$. For each such latent action α we set $\varepsilon = 0.2$ and sampled 500 points from its ε -neighbourhood $N_\varepsilon(\alpha)$. We then fit an affine transformation f_α (Eq. (10)) on 350 randomly selected neighbourhood points and calculated test MSE on the remaining 150 points. We report the average test MSE obtained across all 50 points in Figure 5.

EM policy training For each generative model, introduced in Table 1 and Table 2, we trained one policy with three different random seeds. The average training performance for each of the models is provided in Fig. 6.

Correlation between evaluation metrics and EM policy training We labeled each generative model g with the maximum as well as the average reward achieved during the EM policy training across all three random seeds. We used

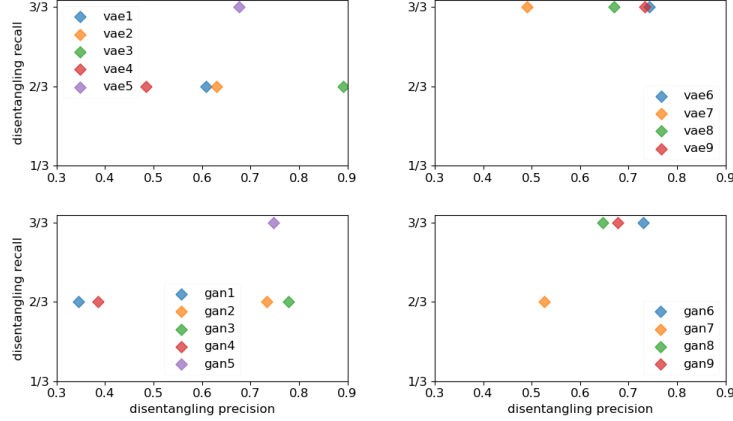


Figure 4: Disentanglement scores.

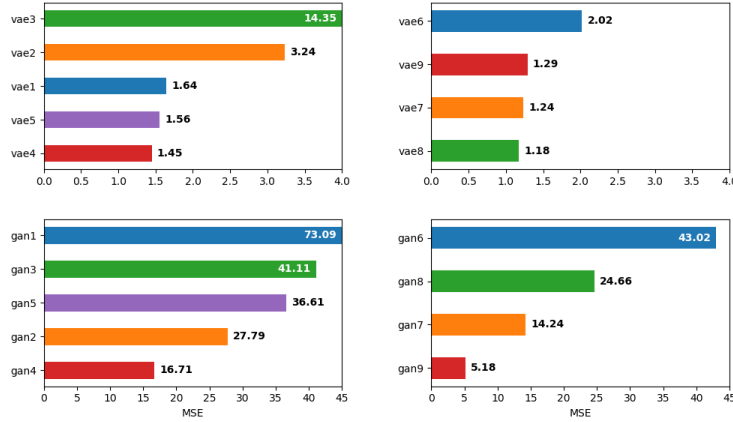


Figure 5: Local linearity test MSE.

automatic relevance determination (ARD) framework to determine the influence of each of the evaluation measures presented in Section 5.2 on the final EM policy training. In particular, we fit an ARD model on the evaluation results obtained in Section 7.3 and report the resulting regression weights in Table 3. We first note that the negative coefficient for the precision metric is a consequence of the experimental results as the generative models in general have a larger precision than the recall (see Figure 3). In future, this can be avoided by a more thorough fine tuning.

Next, we see that for achieving maximum reward, the most important property of generative models is recall followed by precision and then the disentangling precision DiP. The disentangling recall DiR and well as the test MSE error have in this case a low influence on the policy training. On contrary, for average achieved reward, we observe more balanced weights for the pair of precision and recall metrics as well as for the pair of disentangling precision and disentangling recall. Moreover, we see that local linearity can be disregarded.

We conclude that for a successful policy training in the case of the picking task, the generative model should be trained to have high precision and high recall. Moreover, the results imply that the performance of π_θ is not affected by the structure of the latent space measured by disentanglement and local linearity. However, we note that the latent structure can be essential when performing tasks represented by more complex data such that structured latent representations would be beneficial.

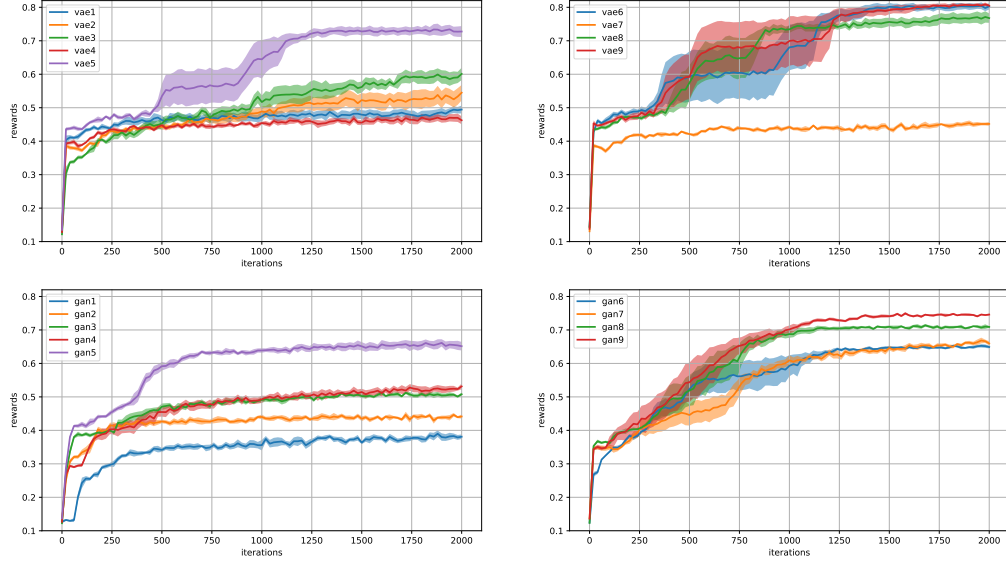


Figure 6: The performance of the policy training

Table 3: ARD regression coefficients (multiplied by 100) corresponding to the evaluation metrics from Section 5.2.

	DiP	DiR	Precision	Recall	Test MSE
max reward	6.585	0.197	-34.468	60.173	0.004
mean reward	7.189	6.217	-23.503	39.905	0.000

7.4 Multi-agent learning

Fig. 7 demonstrates the performance of the EM policy training algorithm for different numbers of variational policies in the E-step. As it is shown, using more than one variational policies in the E-step improves the performance in the beginning of the training. In other words, the RL agent learns faster with more than 4 variational policies for the first 100 iterations. However, still the best performance is achieved by the EM policy training with one variational policy. This observation requires more investigations that is a part of our future work.

8 Conclusion

We presented an RL framework that combined with generative models trains deep visuomotor policies in a data-efficient manner. The generative models are integrated to the RL optimization by introducing a latent variable α that is a low-dimensional representation of motor actions. Using the latent action variable α , we divided the optimization of the parameters Θ of the deep visuomotor policy $\pi_\Theta(\tau|s)$ into two parts: optimizing the parameters ϑ of a generative model $p_\vartheta(\tau|\alpha)$ that generates valid sequences of motor actions, and optimizing the parameters θ of a sub-policy $\pi_\theta(\alpha|s)$, where $\Theta = [\theta, \vartheta]$. The sub-policy parameters θ are found using the EM algorithm, while generative model parameters ϑ are trained unsupervised to optimize the objective corresponding to the chosen generative model. In summary, the complete framework consists of data-efficient three downstream tasks: (1) training the generative model p_ϑ , (2) training the sub-policy π_θ , and (3) supervised end-to-end training the deep visuomotor policy π_Θ .

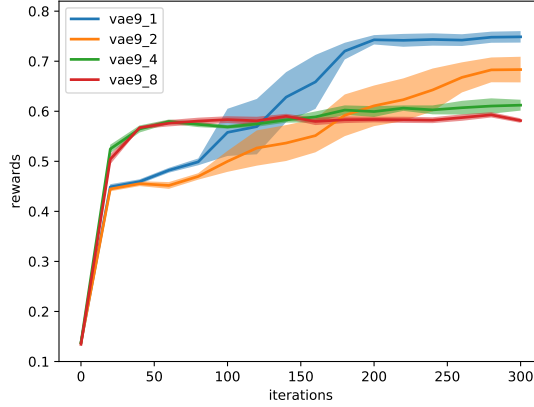


Figure 7: The performance of the EM policy training for 1, 2, 4, and 8 variational policies. The results are provided using the VAE9 generative model.

Moreover, we provided a set of measures for evaluating the quality of the generative models regulated by the RL policy search algorithms such that we can predict the performance of the deep policy training π_Θ prior to the actual training. In particular, we defined two new measures, disentanglement and local linearity, that evaluate the quality of the latent space of the generative model p_θ , and complemented them with precision and recall measure [3] which evaluates the quality of the generated samples. We experimentally demonstrated the predictive power of these measures on a picking task using a set of different VAE and GAN generative models.

Acknowledgments

This work was supported by Knut and Alice Wallenberg Foundation, the EU through the project EnTimeMent, the Swedish Foundation for Strategic Research through the COIN project, and also by the Academy of Finland through the DEEPEN project.

References

- [1] S. Levine, C. Finn, T. Darrell, and P. Abbeel, “End-to-end training of deep visuomotor policies,” *The Journal of Machine Learning Research*, vol. 17, no. 1, pp. 1334–1373, 2016.
- [2] S. Levine, P. Pastor, A. Krizhevsky, J. Ibarz, and D. Quillen, “Learning hand-eye coordination for robotic grasping with deep learning and large-scale data collection,” *The International Journal of Robotics Research*, vol. 37, no. 4-5, pp. 421–436, 2018.
- [3] T. Kynkänniemi, T. Karras, S. Laine, J. Lehtinen, and T. Aila, “Improved precision and recall metric for assessing generative models,” in *Advances in Neural Information Processing Systems*, 2019, pp. 3927–3936.
- [4] M. S. Sajjadi, O. Bachem, M. Lucic, O. Bousquet, and S. Gelly, “Assessing generative models via precision and recall,” in *Advances in Neural Information Processing Systems*, 2018, pp. 5228–5237.
- [5] I. Higgins, L. Matthey, A. Pal, C. Burgess, X. Glorot, M. Botvinick, S. Mohamed, and A. Lerchner, “beta-vae: Learning basic visual concepts with a constrained variational framework,” in *International Conference on Learning Representations*, 2017.
- [6] X. Chen, Y. Duan, R. Houthooft, J. Schulman, I. Sutskever, and P. Abbeel, “Infogan: Interpretable representation learning by information maximizing generative adversarial nets,” in *Advances in neural information processing systems*, 2016, pp. 2172–2180.

- [7] A. Ghadirzadeh, A. Maki, D. Kragic, and M. Björkman, “Deep predictive policy training using reinforcement learning,” in *2017 IEEE/RSJ International Conference on Intelligent Robots and Systems (IROS)*. IEEE, 2017, pp. 2351–2358.
- [8] K. Arndt, M. Hazara, A. Ghadirzadeh, and V. Kyrki, “Meta reinforcement learning for sim-to-real domain adaptation,” *arXiv preprint arXiv:1909.12906*, 2019.
- [9] X. Chen, A. Ghadirzadeh, M. Björkman, and P. Jensfelt, “Adversarial feature training for generalizable robotic visuomotor control,” *arXiv preprint arXiv:1909.07745*, 2019.
- [10] A. Hämäläinen, K. Arndt, A. Ghadirzadeh, and V. Kyrki, “Affordance learning for end-to-end visuomotor robot control,” *arXiv preprint arXiv:1903.04053*, 2019.
- [11] J. Bütepage, A. Ghadirzadeh, Ö. Ö. Karadag, M. Björkman, and D. Kragic, “Imitating by generating: deep generative models for imitation of interactive tasks,” *arXiv preprint arXiv:1910.06031*, 2019.
- [12] C. Finn, X. Y. Tan, Y. Duan, T. Darrell, S. Levine, and P. Abbeel, “Deep spatial autoencoders for visuomotor learning,” in *2016 IEEE International Conference on Robotics and Automation (ICRA)*. IEEE, 2016, pp. 512–519.
- [13] D. Kalashnikov, A. Irpan, P. Pastor, J. Ibarz, A. Herzog, E. Jang, D. Quillen, E. Holly, M. Kalakrishnan, V. Vanhoucke *et al.*, “Qt-opt: Scalable deep reinforcement learning for vision-based robotic manipulation,” *arXiv preprint arXiv:1806.10293*, 2018.
- [14] D. Quillen, E. Jang, O. Nachum, C. Finn, J. Ibarz, and S. Levine, “Deep reinforcement learning for vision-based robotic grasping: A simulated comparative evaluation of off-policy methods,” in *2018 IEEE International Conference on Robotics and Automation (ICRA)*. IEEE, 2018, pp. 6284–6291.
- [15] A. Singh, L. Yang, and S. Levine, “Gplac: Generalizing vision-based robotic skills using weakly labeled images,” in *Proceedings of the IEEE International Conference on Computer Vision*, 2017, pp. 5851–5860.
- [16] C. Devin, P. Abbeel, T. Darrell, and S. Levine, “Deep object-centric representations for generalizable robot learning,” in *2018 IEEE International Conference on Robotics and Automation (ICRA)*. IEEE, 2018, pp. 7111–7118.
- [17] L. Pinto, M. Andrychowicz, P. Welinder, W. Zaremba, and P. Abbeel, “Asymmetric actor critic for image-based robot learning,” *arXiv preprint arXiv:1710.06542*, 2017.
- [18] C. Finn and S. Levine, “Deep visual foresight for planning robot motion,” in *2017 IEEE International Conference on Robotics and Automation (ICRA)*. IEEE, 2017, pp. 2786–2793.
- [19] S. Gu, E. Holly, T. Lillicrap, and S. Levine, “Deep reinforcement learning for robotic manipulation with asynchronous off-policy updates,” in *2017 IEEE international conference on robotics and automation (ICRA)*. IEEE, 2017, pp. 3389–3396.
- [20] S. Dasari, F. Ebert, S. Tian, S. Nair, B. Bucher, K. Schmeckpeper, S. Singh, S. Levine, and C. Finn, “Robonet: Large-scale multi-robot learning,” *arXiv preprint arXiv:1910.11215*, 2019.
- [21] A. Abdolmaleki, S. H. Huang, L. Hasenclever, M. Neunert, H. F. Song, M. Zambelli, M. F. Martins, N. Heess, R. Hadsell, and M. Riedmiller, “A distributional view on multi-objective policy optimization,” *arXiv preprint arXiv:2005.07513*, 2020.
- [22] X. B. Peng, M. Andrychowicz, W. Zaremba, and P. Abbeel, “Sim-to-real transfer of robotic control with dynamics randomization,” in *2018 IEEE international conference on robotics and automation (ICRA)*. IEEE, 2018, pp. 1–8.
- [23] J. Tobin, R. Fong, A. Ray, J. Schneider, W. Zaremba, and P. Abbeel, “Domain randomization for transferring deep neural networks from simulation to the real world,” in *2017 IEEE/RSJ international conference on intelligent robots and systems (IROS)*. IEEE, 2017, pp. 23–30.

- [24] T. Yu, C. Finn, A. Xie, S. Dasari, T. Zhang, P. Abbeel, and S. Levine, “One-shot imitation from observing humans via domain-adaptive meta-learning,” *arXiv preprint arXiv:1802.01557*, 2018.
- [25] X. Chen, A. Ghadirzadeh, J. Folkesson, M. Björkman, and P. Jensfelt, “Deep reinforcement learning to acquire navigation skills for wheel-legged robots in complex environments,” in *2018 IEEE/RSJ International Conference on Intelligent Robots and Systems (IROS)*. IEEE, 2018, pp. 3110–3116.
- [26] E. Tzeng, J. Hoffman, K. Saenko, and T. Darrell, “Adversarial discriminative domain adaptation,” in *Proceedings of the IEEE Conference on Computer Vision and Pattern Recognition*, 2017, pp. 7167–7176.
- [27] E. Tzeng, C. Devin, J. Hoffman, C. Finn, P. Abbeel, S. Levine, K. Saenko, and T. Darrell, “Adapting deep visuomotor representations with weak pairwise constraints,” in *Algorithmic Foundations of Robotics XII*. Springer, 2020, pp. 688–703.
- [28] J. Schulman, S. Levine, P. Abbeel, M. Jordan, and P. Moritz, “Trust region policy optimization,” in *International conference on machine learning*, 2015, pp. 1889–1897.
- [29] J. Schulman, F. Wolski, P. Dhariwal, A. Radford, and O. Klimov, “Proximal policy optimization algorithms,” *arXiv preprint arXiv:1707.06347*, 2017.
- [30] G. Neumann, “Variational inference for policy search in changing situations,” in *Proceedings of the 28th International Conference on Machine Learning, ICML 2011*, 2011, pp. 817–824.
- [31] M. P. Deisenroth, G. Neumann, J. Peters *et al.*, “A survey on policy search for robotics,” *Foundations and Trends® in Robotics*, vol. 2, no. 1–2, pp. 1–142, 2013.
- [32] S. Levine and V. Koltun, “Variational policy search via trajectory optimization,” in *Advances in neural information processing systems*, 2013, pp. 207–215.
- [33] A. Ghadirzadeh, “Sensorimotor robot policy training using reinforcement learning,” Ph.D. dissertation, KTH Royal Institute of Technology, 2018.
- [34] J. Peters and S. Schaal, “Policy gradient methods for robotics,” in *2006 IEEE/RSJ International Conference on Intelligent Robots and Systems*. IEEE, 2006, pp. 2219–2225.
- [35] ———, “Reinforcement learning of motor skills with policy gradients,” *Neural networks*, vol. 21, no. 4, pp. 682–697, 2008.
- [36] A. J. Ijspeert, J. Nakanishi, and S. Schaal, “Learning attractor landscapes for learning motor primitives,” in *Advances in neural information processing systems*, 2003, pp. 1547–1554.
- [37] A. J. Ijspeert, J. Nakanishi, H. Hoffmann, P. Pastor, and S. Schaal, “Dynamical movement primitives: learning attractor models for motor behaviors,” *Neural computation*, vol. 25, no. 2, pp. 328–373, 2013.
- [38] M. Hazara and V. Kyrki, “Transferring generalizable motor primitives from simulation to real world,” *IEEE Robotics and Automation Letters*, vol. 4, no. 2, pp. 2172–2179, 2019.
- [39] T. Haarnoja, V. Pong, A. Zhou, M. Dalal, P. Abbeel, and S. Levine, “Composable deep reinforcement learning for robotic manipulation,” in *2018 IEEE International Conference on Robotics and Automation (ICRA)*. IEEE, 2018, pp. 6244–6251.
- [40] M. Lippi, P. Poklukar, M. C. Welle, A. Varava, H. Yin, A. Marino, and D. Kragic, “Latent space roadmap for visual action planning of deformable and rigid object manipulation,” *arXiv preprint arXiv:2003.08974*, 2020.
- [41] N. Gothoskar, M. Lázaro-Gredilla, A. Agarwal, Y. Bekiroglu, and D. George, “Learning a generative model for robot control using visual feedback,” *arXiv preprint arXiv:2003.04474*, 2020.
- [42] M. Igl, L. Zintgraf, T. A. Le, F. Wood, and S. Whiteson, “Deep variational reinforcement learning for pomdps,” *arXiv preprint arXiv:1806.02426*, 2018.

- [43] L. Buesing, T. Weber, S. Racaniere, S. Eslami, D. Rezende, D. P. Reichert, F. Viola, F. Besse, K. Gregor, D. Hassabis *et al.*, “Learning and querying fast generative models for reinforcement learning,” *arXiv preprint arXiv:1802.03006*, 2018.
- [44] N. Mishra, P. Abbeel, and I. Mordatch, “Prediction and control with temporal segment models,” in *Proceedings of the 34th International Conference on Machine Learning-Volume 70*. JMLR.org, 2017, pp. 2459–2468.
- [45] N. R. Ke, A. Singh, A. Touati, A. Goyal, Y. Bengio, D. Parikh, and D. Batra, “Modeling the long term future in model-based reinforcement learning,” 2018.
- [46] D. Hafner, T. Lillicrap, I. Fischer, R. Villegas, D. Ha, H. Lee, and J. Davidson, “Learning latent dynamics for planning from pixels,” *arXiv preprint arXiv:1811.04551*, 2018.
- [47] N. Rhinehart, R. McAllister, and S. Levine, “Deep imitative models for flexible inference, planning, and control,” *arXiv preprint arXiv:1810.06544*, 2018.
- [48] O. Krupnik, I. Mordatch, and A. Tamar, “Multi agent reinforcement learning with multi-step generative models,” *arXiv preprint arXiv:1901.10251*, 2019.
- [49] A. Brock, J. Donahue, and K. Simonyan, “Large scale gan training for high fidelity natural image synthesis,” *arXiv preprint arXiv:1809.11096*, 2018.
- [50] T.-C. Wang, M.-Y. Liu, J.-Y. Zhu, A. Tao, J. Kautz, and B. Catanzaro, “High-resolution image synthesis and semantic manipulation with conditional gans,” in *Proceedings of the IEEE conference on computer vision and pattern recognition*, 2018, pp. 8798–8807.
- [51] F. Wiewel and B. Yang, “Continual learning for anomaly detection with variational autoencoder,” in *ICASSP 2019 - 2019 IEEE International Conference on Acoustics, Speech and Signal Processing (ICASSP)*, 2019, pp. 3837–3841.
- [52] W. Xu and Y. Tan, “Semisupervised text classification by variational autoencoder,” *IEEE Transactions on Neural Networks and Learning Systems*, vol. 31, no. 1, pp. 295–308, 2020.
- [53] F. Locatello, S. Bauer, M. Lučić, G. Rätsch, S. Gelly, B. Schölkopf, and O. F. Bachem, “Challenging common assumptions in the unsupervised learning of disentangled representations,” in *International Conference on Machine Learning*, 2019, best Paper Award.
- [54] I. Higgins, D. Amos, D. Pfau, S. Racaniere, L. Matthey, D. Rezende, and A. Lerchner, “Towards a definition of disentangled representations,” *arXiv preprint arXiv:1812.02230*, 2018.
- [55] Y. Bengio, A. Courville, and P. Vincent, “Representation learning: A review and new perspectives,” *IEEE Transactions on Pattern Analysis and Machine Intelligence*, vol. 35, no. 8, pp. 1798–1828, 2013.
- [56] H. Kim and A. Mnih, “Disentangling by factorising,” *arXiv preprint arXiv:1802.05983*, 2018.
- [57] C. Eastwood and C. K. Williams, “A framework for the quantitative evaluation of disentangled representations,” 2018.
- [58] T. Q. Chen, X. Li, R. B. Grosse, and D. K. Duvenaud, “Isolating sources of disentanglement in variational autoencoders,” in *Advances in Neural Information Processing Systems*, 2018, pp. 2610–2620.
- [59] I. Jeon, W. Lee, and G. Kim, “IB-GAN: Disentangled representation learning with information bottleneck GAN,” 2019.
- [60] W. Lee, D. Kim, S. Hong, and H. Lee, “High-fidelity synthesis with disentangled representation,” *arXiv preprint arXiv:2001.04296*, 2020.
- [61] B. Liu, Y. Zhu, Z. Fu, G. de Melo, and A. Elgammal, “Oogan: Disentangling gan with one-hot sampling and orthogonal regularization,” 2019.

- [62] T. Salimans, I. Goodfellow, W. Zaremba, V. Cheung, A. Radford, X. Chen, and X. Chen, “Improved techniques for training gans,” in *Advances in Neural Information Processing Systems 29*, D. D. Lee, M. Sugiyama, U. V. Luxburg, I. Guyon, and R. Garnett, Eds. Curran Associates, Inc., 2016, pp. 2234–2242.
- [63] M. Heusel, H. Ramsauer, T. Unterthiner, B. Nessler, and S. Hochreiter, “Gans trained by a two time-scale update rule converge to a local nash equilibrium,” in *Advances in Neural Information Processing Systems 30*, I. Guyon, U. V. Luxburg, S. Bengio, H. Wallach, R. Fergus, S. Vishwanathan, and R. Garnett, Eds. Curran Associates, Inc., 2017, pp. 6626–6637.
- [64] M. Bińkowski, D. J. Sutherland, M. Arbel, and A. Gretton, “Demystifying MMD GANs,” in *International Conference on Learning Representations*, 2018.
- [65] L. Simon, R. Webster, and J. Rabin, “Revisiting precision recall definition for generative modeling,” in *Proceedings of the 36th International Conference on Machine Learning*, ser. Proceedings of Machine Learning Research, K. Chaudhuri and R. Salakhutdinov, Eds., vol. 97. Long Beach, California, USA: PMLR, 09–15 Jun 2019, pp. 5799–5808.
- [66] D. P. Kingma and M. Welling, “Auto-encoding variational bayes,” *International Conference on Learning Representations*, 2014.
- [67] D. J. Rezende, S. Mohamed, and D. Wierstra, “Stochastic backpropagation and approximate inference in deep generative models,” in *Int. Conf. Mach. Learn.*, 2014, pp. 1278–1286.
- [68] I. Goodfellow, J. Pouget-Abadie, M. Mirza, B. Xu, D. Warde-Farley, S. Ozair, A. Courville, and Y. Bengio, “Generative adversarial nets,” in *Advances in neural information processing systems*, 2014, pp. 2672–2680.
- [69] Y. Bengio, A. Courville, and P. Vincent, “Representation learning: A review and new perspectives,” *IEEE transactions on pattern analysis and machine intelligence*, vol. 35, no. 8, pp. 1798–1828, 2013.
- [70] A. Gretton, K. M. Borgwardt, M. J. Rasch, B. Schölkopf, and A. Smola, “A kernel two-sample test,” *Journal of Machine Learning Research*, vol. 13, no. 25, pp. 723–773, 2012.

Appendix A Disentanglement Score

Let $l \in \{1, \dots, N_\alpha\}$ be a fixed latent dimension. In phase 1, we perform $D \in \mathbb{N}$ interventions $\alpha_l = I_d$ on l for $d = 1, \dots, D$. Interventions are chosen from the set of equidistant points on the interval $[-a, a]$ such that $I_d = -a + 2a \cdot \frac{d-1}{D-1}$. The value a is chosen such that $[-a, a]$ is in the support of the prior distribution $p(\alpha)$. Since $p(\alpha)$ is a standard normal distribution in the case of VAEs and a uniform distribution on the interval $[-1, 1]$ in the case of GANs, we set a to be 1.5 and 1 in the case of the VAEs and GANs, respectively. Each intervention $d = 1, \dots, D$ is performed on n samples from the prior distribution $p(\alpha)$ and yields a set of n end states denoted by $\mathcal{S}_g^{l-I_d}$. For each intervention we additionally randomly sample a set \mathcal{S}_r of n end states corresponding to the training motor data. Note that elements of both $\mathcal{S}_g^{l-I_d}$ and \mathcal{S}_r are N_s -dimensional with N_s being the dimension of the end state space.

In phase 2, we calculate the $\text{MMD}(\text{proj}_j \mathcal{S}_g^{l-I_d}, \text{proj}_j \mathcal{S}_r)$ for fixed intervention $d = 1, \dots, D$ and every end state component $j = 1, \dots, N_s$. In order to determine if the difference between the sets $\text{proj}_j \mathcal{S}_g^{l-I_d}$ and $\text{proj}_j \mathcal{S}_r$ is significant, we first perform a permutation test to determine the critical value c_η where η denotes the significance level. We say that the intervention I_d was significant for an end state component j if $\text{MMD}(\text{proj}_j \mathcal{S}_g^{l-I_d}, \text{proj}_j \mathcal{S}_r) > c_\eta$. The calculations in phase 2 were repeated p times with a resampled set of n training end states \mathcal{S}_r . In all our experiments we set $p = 10$ and perform the permutation test 100 times with $\eta = 0.001$.

Therefore, phases 1 and 2 yield functions $c_g : \{1, \dots, N_\alpha\} \rightarrow \{1, \dots, N_s\}$ and $d_g : \{1, \dots, N_\alpha\} \rightarrow \mathbb{R}$ defined by:

$$c_g(l) = \underset{j=1, \dots, N_s}{\text{argmax}} \overline{\text{MMD}} \left(\text{proj}_j \mathcal{S}_g^{l-I_d}, \text{proj}_j \mathcal{S}_r \right) \quad \text{and} \quad d_g(l) = \overline{\text{MMD}} \left(\text{proj}_{c_g(l)} \mathcal{S}_g^{l-I_d}, \text{proj}_{c_g(l)} \mathcal{S}_r \right)$$

where $\overline{\text{MMD}}$ denotes the average MMD score calculated on a subset of $p \cdot D$ performed interventions that were significant. For the sake of simplicity we omit the explicit reference to the model g from the notations and simply write c and d .

In phase 3 we define the final disentanglement score for the generative model g using the functions c and d . Let \mathcal{P} be a subset of $\{d(l) : l = 1 \dots, N_\alpha\}$ containing its largest three elements, and let $\mathcal{R} = \{c(l) : d(l) \in \mathcal{P}\}$ be the set of the corresponding end state components. We define the *Disentanglement Score* DiS as a pair

$$\text{DiS}(g) = (\text{DiP}(g), \text{DiR}(g)) := \left(\sum_{d \in \mathcal{P}} d, \frac{|\mathcal{R}^\neq|}{N_s} \right) \quad (11)$$

where \mathcal{R}^\neq denotes the subset of unique elements of the set \mathcal{R} .

Appendix B Generative models

B.1 Variational Autoencoder

The architecture of the decoder neural network is visualised in Table 4. The encoder neural network is symmetric to the generator with two output linear layers of size N_α representing the mean and the log standard deviation of the approximate posterior distribution. All the models were trained for 10000 epochs with the learning rate fixed to $1e-4$.

B.2 InfoGAN

The architecture of the generator, discriminator and Q neural network parametrizing $Q_\phi(\alpha|\tau)$ are summarised in Tables 4 and 5. All the models were trained for 1000 epochs with the learning rates of the optimizers for the generator and discriminator networks fixed to $2e-4$.

Table 4: Architecture of the generator neural network.

Linear(N_α , 128) + BatchNorm + ReLU
Linear(128, 256) + BatchNorm + ReLU
Linear(256, 512) + BatchNorm + ReLU
Linear(512, 7 · 79)

Table 5: Architecture of the discriminator and Qnet neural networks.

Shared layers	Linear(7 · 79, 256) + ReLU
	Linear(256, 128) + ReLU
discriminator	Linear(128, 1) + Sigmoid
Qnet	Linear(128, 64)
	Linear(64, N_α)